Characteristics of 150 km echoes linked with solar eclipse and their implications to the echoing phenomenon

A. K. Patra,[1] P. Pavan Chaitanya,[2] and D. Tiwari[3]

Received 1 November 2010; revised 4 April 2011; accepted 6 April 2011; published 21 May 2011.

[1] This paper presents a study based on Gadanki radar observations of 150 km echoes made during the solar eclipse of 15 January 2010 that occurred during 1122–1515 IST. Radar echoes were observed only during 1150–1215 IST and 1344–1356 IST linked with the entry and recovery phases of the eclipse, respectively. The most striking observation found is the unusual ascending and descending features of the echoing regions observed during these two time periods. Although these echoes occurred at higher altitudes than those of control days, SNR and spectral width of these echoes are similar to those of the lower echoing region observed on the control days. Further, Doppler velocities suggest the presence of westward electric field unlike those of the control days. Concurrent ionosonde observations showed ascent and descent of the F_1 layer very similar to those observed in the 150 km echoes. These observations and related analysis suggest that the observed echoes were due to the combined action of the electron density gradients and the reduced recombination rate linked with the solar eclipse effect. These observations are first of its kind and elucidate the role of density gradient and recombination rate in the 150 km echoing process.

Citation: Patra, A. K., P. Pavan Chaitanya, and D. Tiwari (2011), Characteristics of 150 km echoes linked with solar eclipse and their implications to the echoing phenomenon, *J. Geophys. Res.*, *116*, A05319, doi:10.1029/2010JA016258.

1. Introduction

[2] The so-called 150 km echoes, the coherent radar echoes coming from the 140–180 km region during daytime, first detected using the Jicamarca radar nearly four and half decades ago [*Balsley*, 1964], continue to puzzle researchers till the free energy sources and the generation mechanism of the echoing phenomenon are identified. They were found to exhibit narrow spectral width (<15 m s^{-1}) [e.g., *Røyrvik and Miller*, 1981] and were associated to field-aligned irregularities (FAI) [*Røyrvik*, 1982]. Fascinating details of these echoes, revealed through high-resolution observations made using the Jicamarca radar [*Kudeki and Fawcett*, 1993] are (1) height-time variation of the echoing region displaying forenoon descent and afternoon ascent indicating the role of solar zenith angle on the echoing process, (2) quasiperiodic variation in the echo power indicating the possible role of gravity waves in the echoing process, and (3) good correlation of the radial Doppler velocities to ground magnetic field variation suggesting their usefulness in estimating F region $\mathbf{E} \times \mathbf{B}$ drift.

[3] Now we know that these echoes are detected by much smaller radars than that of Jicamarca from other equatorial locations (Ivory Coast, Pohnpei, São Luís, Christmas Island) [*Blanc et al.*, 1996; *Kudeki et al.*, 1998; *de Paula and Hysell*, 2004; *Tsunoda and Ecklund*, 2008] and also from off the magnetic equator, such as those reported from Gadanki in India (13.5°N, 79.2°E, 6.4°N mag. lat.) and Kototabang in Indonesia (0.2°S, 100.32°E, 10.36°S mag. lat.) [e.g., *Choudhary et al.*, 2004; *Patra and Rao*, 2006; *Patra et al.*, 2008]. These observations were made using radar beam oriented perpendicular to earth's magnetic field and clearly demonstrated their potential to study daytime $\mathbf{E} \times \mathbf{B}$ drift at other longitude sectors.

[4] *Chau* [2004], using the Jicamarca radar, however, found that echoes from 150 km region can also be observed with radar beam a few degrees away from perpendicular to earth's magnetic field and in that case the echoes display spectral shape similar to the expected incoherent scatter spectra, but with 1–2 orders of magnitude enhancement. Such observations, however, have so far been limited to Jicamarca and appear to be closely linked with incoherent scattering process.

[5] In this paper, we present interesting new results of 150 km echoes made using the Gadanki radar during the solar eclipse of 15 January 2010, which occurred during 1122–1515 IST (Indian Standard Time = UT + 5.5 h), and discuss these new results in conjunction with concurrent ionosonde observations in advancing our understanding on the enigmatic 150 km echoing phenomenon reported from several equatorial/low-latitude radar observatories.

2. A Brief Observational Overview

[6] The solar eclipse of 15 January 2010 occurred over Gadanki during 1122–1515 IST with its maximum effectiveness at 1328 IST. It was an annular one with obscuration

[1]National Atmospheric Research Laboratory, Gadanki, India.
[2]Department of Physics, Sri Venkateswara University, Tirupati, India.
[3]Indian Institute of Geomagnetism, Navi Mumbai, India.

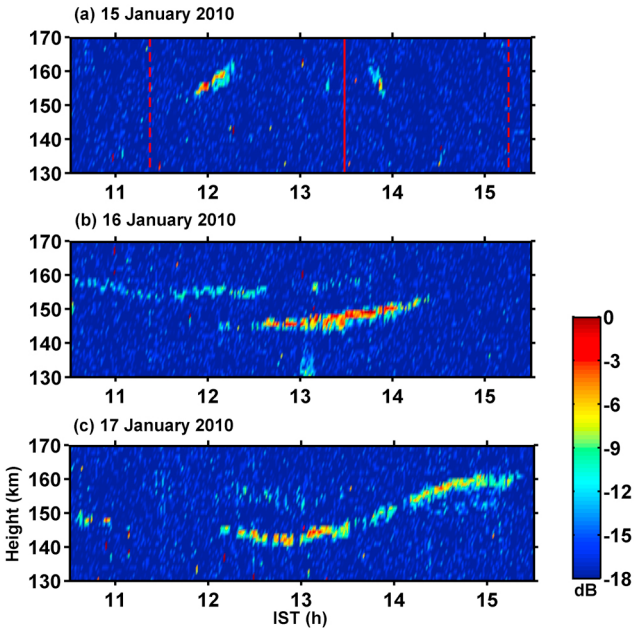

Figure 1. Height-time-SNR maps of 150 km echoes observed on (a) 15 January, (b) 16 January, and (c) 17 January 2010. In Figure 1a, the two dotted lines represent the duration of the eclipse, and the solid line represents the time of maximum obscuration.

of 79.4% and magnitude of 0.864. To study various aspects of atmosphere-ionosphere response to the solar eclipse, the Gadanki MST radar was operated during 13–17 January 2010. In order to meet various scientific needs, the radar experiments were conducted with three beams ($East_{14}$, Zenith, and $North_{14}$, where the suffix represents the off-zenith angle) to obtain wind information in the troposphere-stratosphere-mesosphere region and to observe the E and 150 km region FAI in quick succession. It should be mentioned that due to the finite beam width of the antenna radiation pattern (half power full width = 3°), the $North_{14}$ beam satisfies perpendicularity to earth's magnetic field to observe the E and 150 km region FAI echoes. Observations were made with a pulse width of 8 μs, an IPP of 1.3 ms, number of coherent integration of 24, and number of FFT points of 512. Power spectrum data with a unambiguous velocity window of ±45 m s^{-1} and a velocity resolution of 0.18 m s^{-1} were collected from the height region of 2.4–182.4 km with a range resolution of 1.2 km and a time resolution of 21 s. Since the ionospheric FAI observations were taken in one out of three beams, time resolution of FAI observations was 63 s.

[7] Out of the 5 days (13–17 January) of radar observations, 150 km echoes could be noted only on 3 days (15–17 January). For the present study, we will focus on the observations made on 15 January (eclipse day) and use the observations made on 16 and 17 January (control days) for comparison.

3. Observational Results

[8] Figures 1a–1c show the height-time SNR maps of 150 km echoes observed on 15 January, 16 January, and 17 January 2010, respectively. The occurrence period (vertical dotted lines) and the time of maximum obscuration (vertical solid line) of the eclipse are shown in Figure 1a. As is clearly evident from Figure 1, on 15 January there are two patches of 150 km echoes, one occurring during 1150–1215 IST displaying ascending pattern and another during 1344–1356 IST displaying descending pattern, which are strikingly different from those observed on 16 and 17 January. It may also be noted that 150 km echoes did not commence in the morning of 15 January unlike on 16 and 17 January, instead they started occurring nearly 28 min after the commencement of the solar eclipse. The echoing region, however, lasted only for 25 min. It is also important to note that no echo was detected during the main phase of the eclipse. Again, echoes appeared at 1344 IST during the recovery phase and lasted only for 12 min. Echo strength in this patch also was somewhat weaker than those observed during 1150–1215 IST. It is important to mention that *Patra and Rao* [2007] found the 150 km echoes to occur more in the forenoon than in the afternoon. They also found that in the winter season, which includes January and thus relevant for the present study, echo SNR is higher in the forenoon than in the afternoon. Thus the asymmetries in the 1150–1215 IST and 1344–1356 IST observations appear to be linked with the forenoon-afternoon asymmetry of 150 km echoes reported earlier by *Patra and Rao* [2007]. It is interesting to note that the echoes occurred only for brief periods during the entry and recovery phases. No echo condition observed at other times on 15 January as against 16 and 17 January suggests that the ionospheric conditions on 15 January possibly were not conducive for the irregularity generation. As far as quasiperiodicity in the echo occurrence is concerned, although it is not so clear in the SNR maps, a close look of SNR data clearly suggests the presence of 6–15 min periodicity. On 16 and 17 January, the periods are found to be 10–15 min and 6–10 min in the lower and upper echoing regions, respectively. On 15 January, although the echoes were observed for short periods, we noted that two SNR peaks in the first echoing patch are separated by ~10 min, which also falls in the above range.

[9] In addition to the occurrence characteristics of the echoes observed on 15 January, it is equally interesting to note SNR of these echoes. Note from Figure 1 that both on 16 and 17 January, there are two distinct echoing regions and SNR values of the lower echoing region is ~5 dB higher than those of the upper one. It is interesting to note that on 15 January, although echoes occurred at altitudes between 152 and 162 km, SNR of these echoes are stronger than those occurred in the similar height region on 16 and 17 January. Instead, they are found to be similar to those of the lower echoing region (that occurred below 150 km) observed during similar local time on 16 and 17 January.

[10] In order to understand these echoes better, we examined the spectral characteristics and spectral parameters, which are presented in Figures 2 and 3. Figures 2a and 2b illustrate self normalized Doppler power spectra of the echoes observed at 1158:50 IST and 1351:39 IST, respectively. It may be mentioned that the spectral peaks in the top range gate in Figure 2a correspond to noise (due to self normalization). Positive (negative) Doppler frequency represents irregularity drift toward (away from) the radar. As is evident, the Doppler shifts are positive, representing FAI motion downward/southward in the case of Gadanki radar. Although

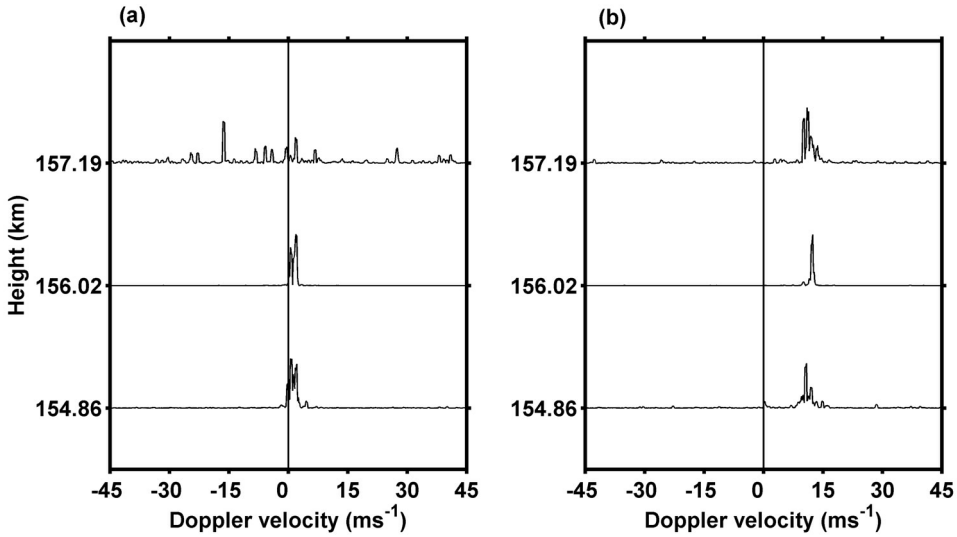

Figure 2. Doppler spectra observed at (a) 1158:50 IST and (b) 1351:39 IST on 15 January 2010.

such Doppler shifts have been observed before [*Patra and Rao*, 2007], their occurrence frequency is low. The spectra are narrow as expected and are very similar to those reported earlier [*Choudhary et al.*, 2004; *Patra and Rao*, 2006]. Figures 3a and 3b show height profiles of average SNR and spectral width observed during 1200–1215 IST on 15 January and during 1215–1300 IST on 16 and 17 January, respectively. It is very clear that both SNR and spectral width observed at 152–162 km region on 15 January are similar to those of the lower echoing region and larger than those of the upper echoing region observed on 16 and 17 January.

[11] In order to compare the velocities with other days of observations, we show the time variations of height-averaged Doppler velocity observed during 1100–1400 IST in Figure 4. Velocities are presented using circle, triangle, and square corresponding to the observations of 15 January, 16 January, and 17 January, respectively. Positive (negative) velocity represents FAI drift upward/northward (downward/southward). It is very clear that on 15 January, the velocities are either close to zero or downward/southward (-12 m s^{-1}) unlike those observed on the other 2 days (2–18 m s^{-1}). The downward/southward velocities observed on 15 January indicate the presence of westward electric field on that day. Here, it may be important to recall from past observations [*Chau and Kudeki*, 2006; *Patra and Rao*, 2007] that the magnitude and polarity of zonal electric field do not play any role in the 150 km echo occurrence and thus the echo occurrence for the two brief periods observed on 15 January, unlike for longer periods on other 2 days, should not be linked to the westward electric field present on that day.

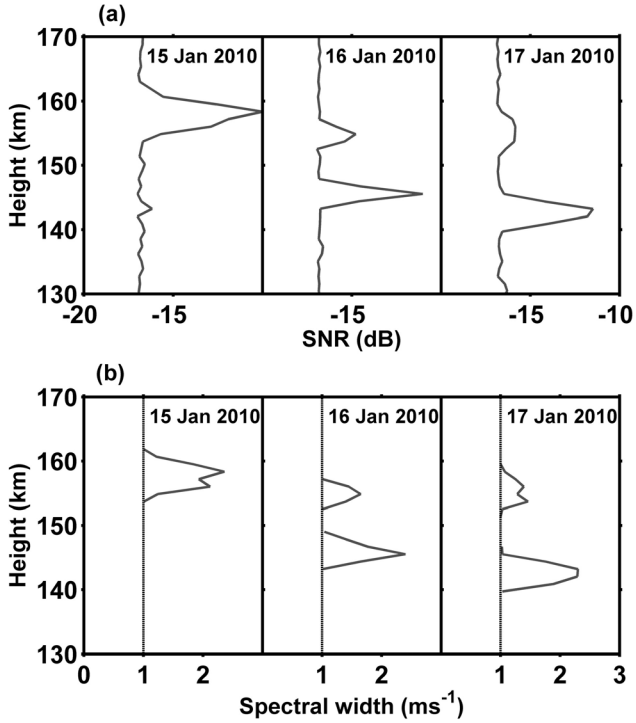

Figure 3. Height profiles of (a) average SNR and (b) average spectral width observed during 1200–1215 IST on 15 January and during 1215–1300 IST on 16 and 17 January.

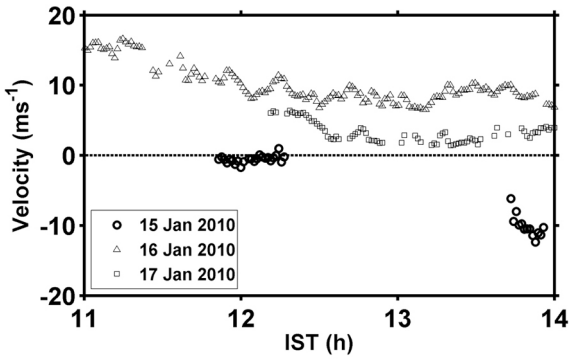

Figure 4. Height-averaged Doppler velocity observed during 1100–1400 IST on 15 January (circle), 16 January (triangle), and 17 January 2010 (square).

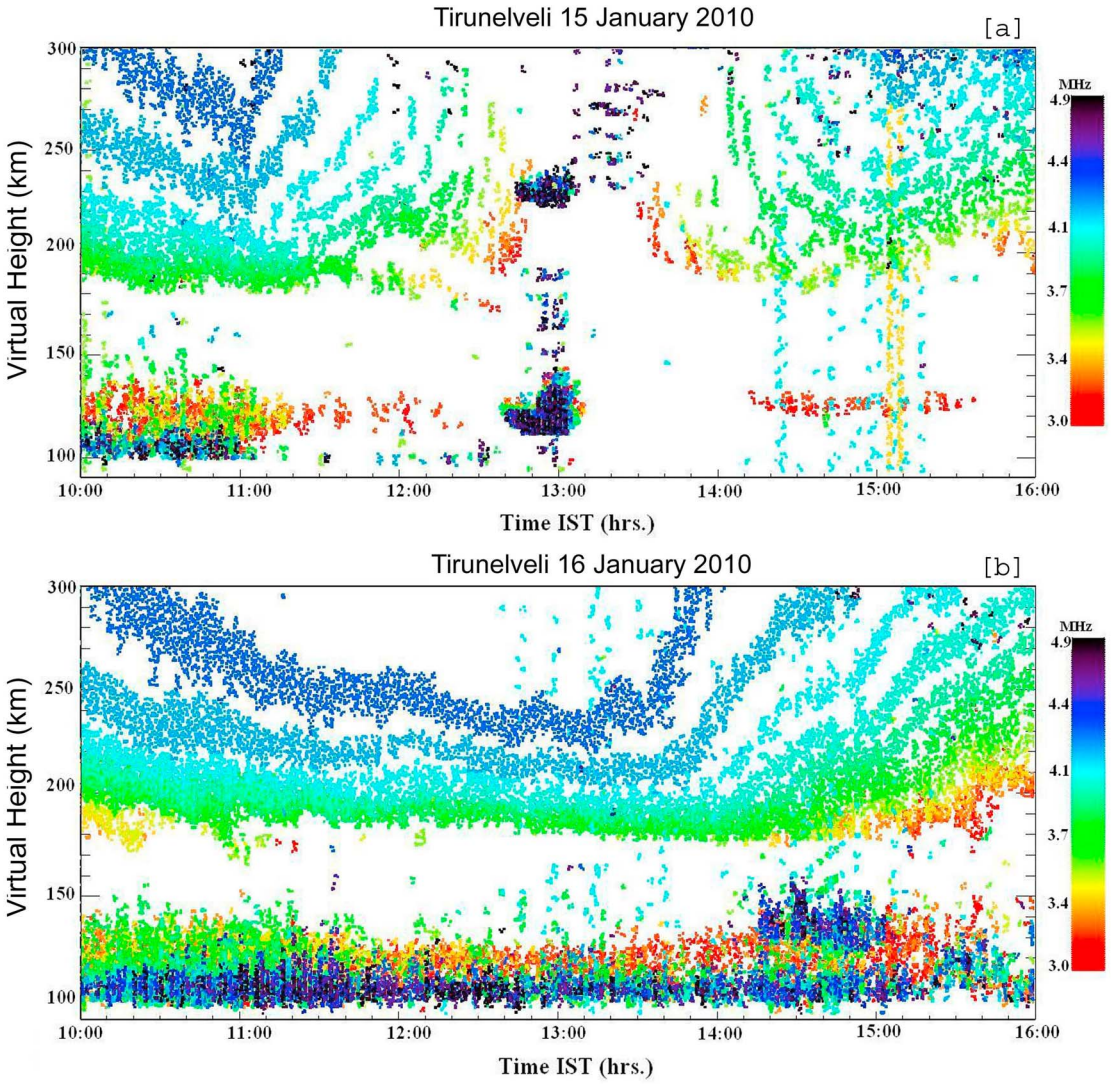

Figure 5. Variations of reflected radio wave frequency as a function of virtual height and time observed using the Tirunelveli ionosonde on (a) 15 January and (b) 16 January 2010.

[12] Considering that the E and F_1 region electron density gets reduced significantly during solar eclipse [*Van Zandt et al.*, 1960], we examined the ionosonde observations made from Tirunelveli (8.7°N, 77.8°E, 0.7° mag. lat.) to study the type of changes occurred in the electron density on the 15 January eclipse event. At Tirunelveli the maximum effectiveness of the solar eclipse was at 1317 IST. Figures 5a and 5b illustrate variations in the reflected radio wave frequency as a function of virtual height and time observed on 15 and 16 January, respectively. Since we are mainly interested in the E and F_1 layer variations, not in the F_2 layer, Figures 5a and 5b are limited to a virtual height of 300 km for the sake of clarity. It should be mentioned that on both days, the virtual height of the F_2 layer ($h'F_2$) was >300 km (which can be seen in the ionograms shown in Figures 6 and 7). Frequency can be translated into electron density using the relation $f = 9000\sqrt{n}$, where f is the radio frequency in Hz and n is the electron density in electrons/cm^3. Figure 5a clearly shows the reduction of E and F1 region density during the eclipse in contrast to those observed on 16 January (Figure 5b) as expected [*Van Zandt et al.*, 1960]. E region echoes observed during 1240–1310 IST on 15 January are due to blanketing E_s activity. Figure 5a clearly shows reduction in the F_1 layer electron density as a function of obscuration and ascending (descending) pattern in the F_1 layer echoing height during the entry (recovery) phase. Also, F_1 layer was not observed during the main phase of the eclipse. Figure 5a also shows some asymmetry during the entry and recovery phases both in terms of height and density of the F_1 layer. Importantly, one can note from Figure 5a a descending layer structure during the entry phase, which is missing during the recovery phase. It may be recalled that the ascending and descending patterns of the radar echoes observed during 1150–1215 IST and 1344–1356 IST, respectively, agreed so well with those observed for the F_1 layer. Further, from Figures 5a and 5b, it is evident that the F_1 layer echoes during those two time periods were at higher altitude on 15 January than on 16 January, which is consistent with those of radar observations of 150 km echoes.

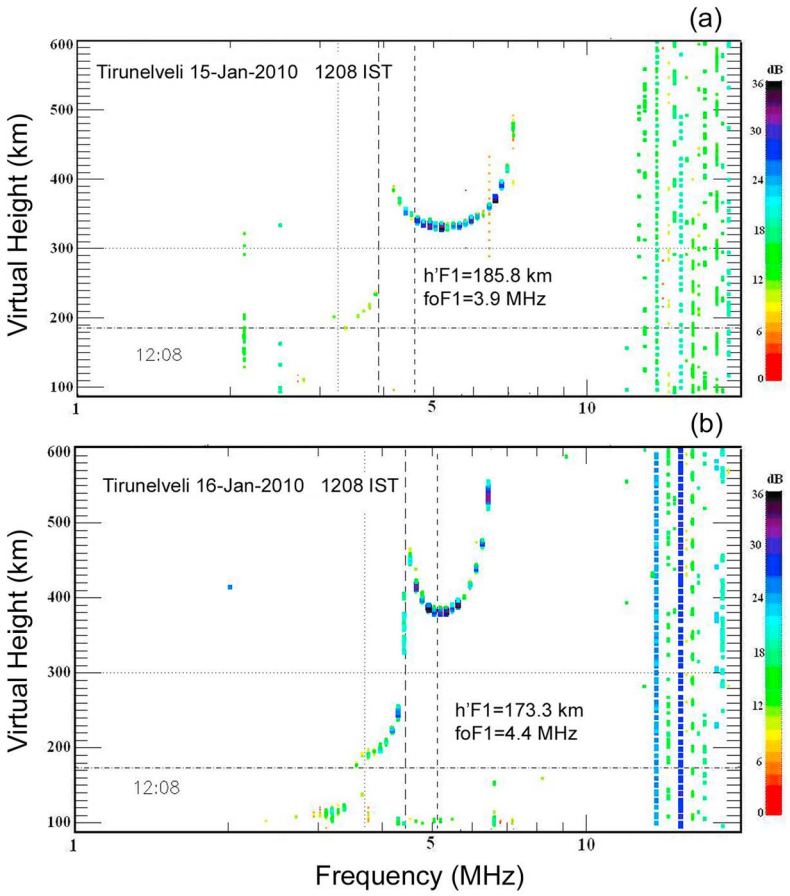

Figure 6. Ionograms observed at 1208 IST on (a) 15 January and (b) 16 January 2010 to demonstrate the changes in the F_1 layer behavior. The bottom horizontal line and middle vertical line represent $h'F_1$ and f_oF_1, respectively.

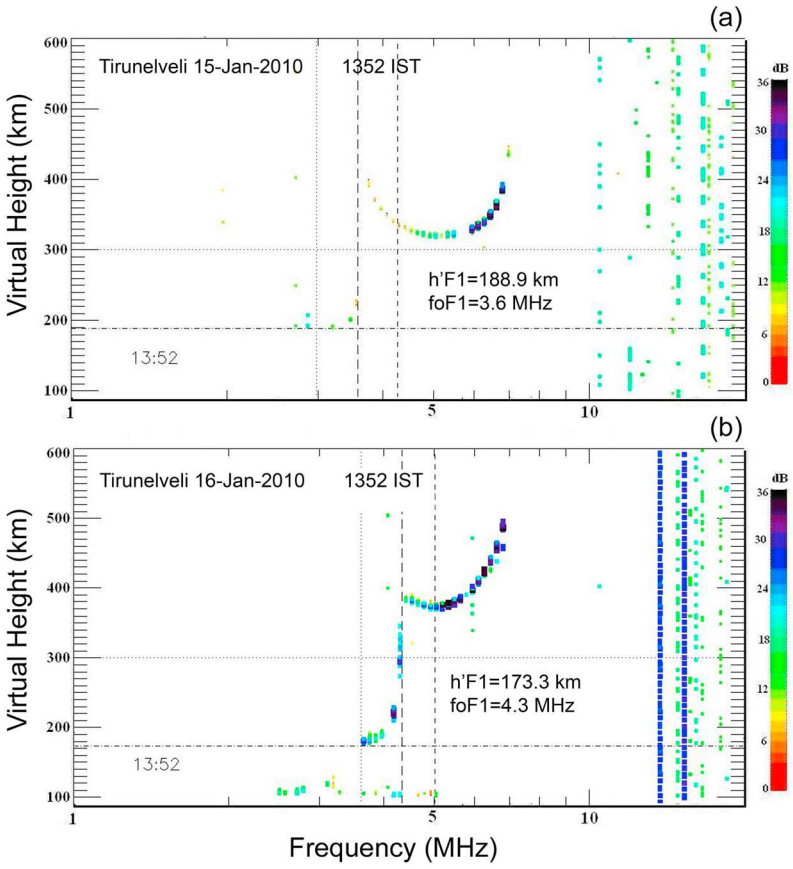

Figure 7. Same as Figure 6 but for ionograms observed at 1352 IST on (a) 15 January and (b) 16 January 2010.

[13] To illustrate the F_1 layer properties observed at 1208 IST and 1352 IST observed on 15 and 16 January, ionograms are presented in Figures 6 and 7, respectively. Figures 6 and 7 clearly show that h'F_2 is >300 km and the virtual height of the F_1 layer (h'F_1) is <200 km. The bottom horizontal line and middle vertical line represent h'F_1 and f_oF_1 (the peak frequency reflected from the F_1 layer), respectively. From Figures 6a and 6b one can note that on 15 January, h'F_1 was 185.8 km, while on 16 January, it was 173.3 km, which implies a rise of 12.5 km in h'F_1 due to solar eclipse effect. Although it is difficult to estimate true heights due to vast difference in the ionospheric conditions below the F_1 layer on those 2 days, they would approximately be ~160 km (for h'F_1 = 185.8 km) and ~150 km (for h'F_1 = 173.3 km). From these ionograms, one can also note a drop of 0.5 MHz (i.e., 4.4 MHz on 16 January to 3.9 MHz on 15 January) in f_oF_1, which implies a drop of electron density by 0.5×10^5 electrons/cm^3 (i.e., from 2.4×10^5 electrons/cm^3 to 1.9×10^5 electrons/cm^3). As regard to the observations made at 1352 IST, from Figures 7a and 7b one can note that h'F_1 was 188.9 km (~3 km higher than that of 1208 IST) on 15 January and 173.3 km (same as that of 1208 IST) on 16 January; and foF1 was 3.6 MHz (0.3 MHz lower than that of 1208 IST) on 15 January and 4.3 MHz (0.1 MHz lower than that of 1208 IST) on 16 January. It is interesting to note that while h'F_1 and f_oF_1 observed at 1208 IST and 1352 IST on 16 January were identical, it is not so for 15 January observations. On 15 January, h'F_1 was higher by 12.5 km at 1208 IST and 15.6 km at 1353 IST; and f_oF_1 was lower by 0.5 MHz at 1208 IST and by 0.7 MHz at 1352 IST than those observed on 16 January. These clearly indicate the presence of asymmetric features in h'F_1 and f_oF_1 observed at 1208 IST and 1352 IST on 15 January. Considering the difference observed in the 150 km echoes during 1150–1215 IST and 1344–1356 IST on 15 January and the fact that 150 km echoes also have forenoon-afternoon asymmetry [*Patra and Rao*, 2007], the present ionosonde observations are of significance, which we will discuss in detail in section 4.

4. Discussion

[14] First of all it is very clear from the observations that while the basic features of the 150 km echoes (e.g., SNR and spectral characteristics) observed on the eclipse day are found to be identical to those observed on the control days; there are striking observations in the 150 km echoes and concurrent ionosonde observations of the F_1 layer, which could be used to understand the physical processes governing them. The important observations linked with the 15 January solar eclipse event are (1) similar ascending/descending pattern in the radar observations of 150 km echoing region and in the concurrent ionosonde observations of the F_1 layer; (2) similar asymmetric behaviors in

the 150 km echoes (occurrence and SNR) and in the F_1 layer properties (h'F_1 and f_oF_1) observed during 1150–1215 IST and 1344–1356 IST; (3) occurrence of 150 km echoes only during two brief periods of ascending and descending phases of the F_1 layer linked with the entry and recovery phases of the eclipse, not during the main phase of the eclipse; (4) the height range of the 150 km echoes on the eclipse day was ~10 km higher than those of the lower echoing region on the control days and similar difference in the F_1 layer height during those time periods; and (5) the spectral parameters (SNR and spectral width) of the echoes observed during the eclipse were similar to those of lower echoing layer observed on the control days.

[15] As far as the control day features are concerned, 150 km echoing regions displayed it's well-known feature of forenoon descent and afternoon ascent [*Kudeki and Fawcett*, 1993], and variation in h'F_1, seen in ionosonde observations, also showed similar trend depicting the solar zenith angle dependence of the F_1 layer behavior. Thus the ascending and descending patterns of the 150 km echoes observed during 1150–1215 IST and 1344–1356 IST and similar features in the ionosonde observations of F_1 echoes are remarkably different from those of the control day features. The one-to-one correspondence between the 150 km echoes and the ionosonde observations of the F_1 layer, in terms of ascending/descending features, on the eclipse day as well as on the control day is striking. Further the striking asymmetry observed in h'F_1 and f_oF_1 on 15 January clearly suggests a close linkage between the two. We believe that the observations during the solar eclipse, presented here, would provide interesting clue in furthering this linkage. We evaluate these in detail later.

[16] As far as solar eclipse effect on the ionospheric density is concerned, one would expect reduction in the electron density due to the domination of recombination processes over photoionization owing to the decrease in incoming radiation during solar eclipse. The molecular ions, however, get recombined faster than the atomic ions due to their higher recombination coefficients (of the order of 10^{-7}cm^3 s^{-1}) than those of atomic ions (of the order of 10^{-12} cm^3 s^{-1}). Since molecular ions, such as NO^+ and O_2^+, are the predominant ions in the E and F_1 region and their density peaks around 150 km and thereafter decreases with increasing height, it is expected that E and F_1 region density will be reduced depending on the degree of sun's obscurity. Thus the ionosonde observations of F_1 echoing pattern on 15 January indicate the gradual bite out and subsequent refilling of electron density at the bottom of the F_1 layer owing to the solar eclipse effect as expected [*Van Zandt et al.*, 1960].

[17] It is interesting to note that the 150 km echoing height appears to be just below the bottom of the F_1 layer (as observed by ionosonde). Further, when we look at all the 5 days of observations carefully, we find that the observations on 15 January, except for the two brief periods (1150–1215, and 1344–1356 IST), are similar to those of 2 previous days (i.e., 13 and 14 January), while the features of the echoing regions observed during the two brief periods are very dissimilar to those of 2 subsequent days (i.e., 16 and 17 January). All these indicate that ionospheric conditions on 15 January most likely were not conducive for the generation of FAI if the changes in the background ionosphere were not brought in by the solar eclipse. The likely factors which might have engendered the generation of irregularities are the density gradient and the reduced value of recombination rate owing to the reduction of plasma density caused by the solar eclipse. The fact that the echoes were observed only for two brief periods on 15 January (not even during the main phase of the solar eclipse), we surmise that the density gradient must be a crucial factor and the critical density gradients were possibly achieved only during those two brief periods and at those heights. In the following we discuss these aspects in more details.

4.1. Link Between 150 km Echoes and F_1 Layer Density Gradient

[18] Although *Balsley* [1964] postulated a causal relationship between the 150 km echoes and the density gradient associated with the F_1 layer, *Tsunoda and Ecklund* [2004] were the first who, by comparing the height-time variation of the 150 km echoes and the density gradient associated with the model electron density profile of the F_1 layer as a function of solar zenith angle [*Dymek*, 1980], suggested that these echoes are possibly generated on the density gradient region in the bottomside F_1 layer.

[19] As far as the present observations are concerned, we first evaluate whether the observed rise in h'F_1 on 15 January was consistent with solar eclipse effect as follows. Considering that sun's obscuration was 20% at 1208 IST and solar flux throughout the solar disk was uniform (which may not be true, but an assumption for convenience), we can consider that only 80% of solar flux was available at that time. Since the height of the F_1 layer has solar zenith angle dependence, we can translate the reduced flux into it's another solar zenith angle equivalent. In fact *Carlson et al.* [1970], using Arecibo radar observations on a solar eclipse, found that the bottomside electron density profile decreased from the preeclipse to the posteclipse period by an amount appropriate to the change in solar zenith angle. In the present case, the zenith angle, χ corresponding to the reduced solar flux of 80% is calculated to be 36°. We found that observed height rise of the bottom of the F_1 layer is ~10 km while the reduction in electron density is 0.5×10^5 electrons/cm^3. The observed density reduction and height rise in the F_1 layer during the solar eclipse reported here are found to be very similar to the model values corresponding to 30° zenith angle reported by *Dymek* [1980]. These results are also consistent with those observed by *Adeniyi and Radicella* [1997]. *Adeniyi and Radicella* [1997] showed that the local time variations in the height and electron density of the F_1 layer were closely related to the solar zenith angle (χ). More importantly, the height migration of the maximum density gradient region at the bottom of the F_1 layer (which occur during 8–17 LT) shown by *Adeniyi and Radicella* [1997, Figure 3] agrees extremely well with that of the 150 km echoes.

[20] In this context, observations of thin electron density layers in the altitude range of 130–200 km, revealed through Jicamarca incoherent scatter measurements [*Chau and Woodman*, 2005] are interesting. *Chau et al.* [2010], by reexamining these observations, found persistence of these thin electron density layers in the 150 km echoing region and also some temporal structures in those layers. Although a correlation study of these structures and 150 km echoes has

not been made yet, we believe that it would be an important step forward to understand the origin of the 150 km echoes.

[21] In the light of the above discussion, we have a good reason to consider the density gradient at the bottom of the F_1 region as an important component in the 150 km echoing phenomenon. The distinct features of the 150 km echoes and concurrent ionosonde observations on the eclipse day essentially support this viewpoint. Furthermore, the detailed differences observed in the F_1 layer observed during the entry and recovery phases and a descending-type layer structure during the entry phase are in support of the differences observed in the 150 km echoes during 1150–1215 IST and 1344–1356 IST. These imply that special type of density gradients, required for the growth of the irregularities, occurred only during those two brief periods. It is quite likely that the density gradients involved had both vertical and horizontal components. More investigations would be required to know the true nature of the gradients and their origin, which gave rise to the irregularities during those two brief periods.

4.2. Generation Mechanism of the Irregularities

[22] As for the generation mechanism of these irregularities, originally two proposals were made: (1) gravity wave wind driven interchange instability [*Kudeki and Fawcett*, 1993] and (2) Kelvin-Helmholtz type instability driven by vertical shear of zonal drift [*Tsunoda*, 1994]. The Kelvin-Helmholtz instability, proposed by *Tsunoda* [1994], however, has not gained much importance considering that no appreciable vertical shear in the zonal flow has been measured [*Røyrvik*, 1982; *Chau and Woodman*, 2004]. Thus interchange instability of some kind, where plasma with a density gradient is stirred, has been repeatedly invoked by several investigators to account for the echoing irregularities [*Tsunoda and Ecklund*, 2000, 2007; *Choudhary et al.*, 2004; *Patra and Rao*, 2007]. Considering the confinement of these echoes to a narrow range of zenith angle, *Tsunoda and Ecklund* [2007] suggested that the density gradients responsible for the generation of the irregularities may be present in the form of tilted sheet-like structures. They may be formed by gravity waves [*Kudeki and Fawcett*, 1993] or by polarization electric field of E region origin through Es layer instability [*Cosgrove and Tsunoda*, 2002] as proposed by *Tsunoda and Ecklund* [2004]. Then the vertical electric field and/or zonal neutral wind would be able to destabilize these density gradient structures through an interchange instability. It may be mentioned that irregularity occurrence is independent of zonal electric field [*Chau and Kudeki*, 2006; *Patra and Rao*, 2007].

[23] *Kudeki and Fawcett* [1993] examined the growth perspective of an interchange instability. Assuming that dissociative recombinational damping is dominant in the 150 km echoing region, *Kudeki and Fawcett* [1993] estimated the pertinent time scale for the instability growth to be 24–42 s. Considering wind as a driving force for density gradient becoming unstable they proposed that this time scale should be less than L/U, where L is the scale length of plasma density and U is the cross-field neutral wind. If we assume U to be 50 m s^{-1}, the gradient scale is estimated to be 1200–2100 m. Taking the electron density profile shown by *Chau and Woodman* [2005] as reference, it looks that it is quite realistic to get required gradient scales for the growth of an interchange instability. The fact that the 150 km echoes observed on 15 January were linked with low background density due to solar eclipse effect, the recombination rate applicable was also lower than that of normal condition. This implies that the recombination time scale must be remarkably higher than that used by *Kudeki and Fawcett* [1993], resulting in higher growth rate of the interchange instability to account for the observed 150 km echoes on 15 January.

[24] In this context, it may be worth visiting the radar observations of nighttime irregularities in the same height region, displaying descending echoing layer and narrow spectral features (<30 m s^{-1}), which have been linked to intermediate layers [e.g., *Patra et al.*, 2002]. It may be mentioned that SNR of such echoes are 12 dB lower than their E region counterpart. Although these irregularities have relatively large SNR and spectral width when compared to daytime 150 km echoes, which is understandable considering the differences in the ionospheric conditions and growth rate of the instability during the day and night, it may be worth considering these irregularities in an effort to understand the physical processes that would generate irregularities in the 150 km region. The important differences between day and night conditions that one would expect are relatively weak density gradient and one order larger background density during daytime than those of nighttime. This implies that the time scale for the growth of the same instability as proposed by *Kudeki and Fawcett* [1993] would be 2–4 s. This means that plasma instability would grow 10 times faster and could lead to nonlinearity giving rise to enhanced turbulence activity. The observed spectral width and SNR for the nighttime echoes reported by *Patra et al.* [2002] seem to be quite consistent with those expected from the above argument. Although intermediate layer's features have not been observed so far in the 150 km echoing layers, such features, if found, would make an important step forward in understanding the underlying physical processes responsible for irregularity generation in the 150 km height region. We, however, believe that density gradients associated with ion layers formed through wind shear action is not essential considering that they do not occur at the magnetic equator, but the 150 km echoes do. They, however, may play some role at latitudes like Gadanki, which we are yet to examine.

5. Concluding Remarks

[25] We have presented unique observational features of 150 km echoes captured during the solar eclipse and argued that the combined action of electron density gradient and reduced recombination rate, provided through the effect of solar eclipse, was responsible for the excitation of the irregularities manifesting radar echoes. The fact that the 150 km echoes were observed during two brief periods, the required conditions for the generation of the irregularities were achieved during those two periods only. We surmise that the critical conditions were linked with the density gradients and the recombination rates during those two periods. We also argued that an interchange instability of the kind proposed by *Kudeki and Fawcett* [1993] is capable of generating these irregularities. High-resolution in situ measurements of electron density profile are essential to verify the above inference and also to examine the growth rate of an interchange

instability explaining the origin of the puzzling 150 km echoes.

[26] **Acknowledgments.** The observations reported were made during the solar eclipse campaign under the CAWSES-India program. Authors gratefully acknowledge NARL and IIG technical staff for making the observations reported. Authors also gratefully acknowledge both the reviewers for their valuable comments and suggestions for the improvement of the paper.

[27] Robert Lysak thanks Eurico de Paula and another reviewer for their assistance in evaluating this paper.

References

Adeniyi, J. O., and S. M. Radicella (1997), Electron density and height at the F_1 region minimum gradient at low solar activity for an equatorial station, *Radio Sci.*, *32*, 1867–1874, doi:10.1029/96RS03639.

Balsley, B. B. (1964), Evidence of stratified echoing region at 150 km in the vicinity of magnetic equator during daylight hours, *J. Geophys. Res.*, *69*, 1925–1930, doi:10.1029/JZ069i009p01925.

Blanc, E., B. Marcandalli, and E. Houngninou (1996), Kilometric irregularities in the *E* and *F* regions of the daytime equatorial ionosphere observed by a high resolution HF radar, *Geophys. Res. Lett.*, *23*, 645–648, doi:10.1029/96GL00415.

Carlson, H. C., R. Harper, V. Wickwar, R. L. Showen, R. Behnke, T. F. Trost, L. R. Cogger, and C. J. Nelson (1970), Eclipse observations at Arecibo, Puerto Rico, on March 7, 1970, *Nature*, *226*, 1124–1125, doi:10.1038/2261124a0.

Chau, J. L. (2004), Unexpected spectral characteristics of VHF radar signals from 150-km region over Jicamarca, *Geophys. Res. Lett.*, *31*, L23803, doi:10.1029/2004GL021620.

Chau, J. L., and E. Kudeki (2006), Statistics of 150-km echoes over Jicamarca based on low-power VHF observations, *Ann. Geophys.*, *24*, 1305–1310, doi:10.5194/angeo-24-1305-2006.

Chau, J. L., and R. F. Woodman (2004), Daytime vertical and zonal velocities from 150-km echoes: Their relevance to *F*-region dynamics, *Geophys. Res. Lett.*, *31*, L17801, doi:10.1029/2004GL020800.

Chau, J. L., and R. F. Woodman (2005), *D* and *E* region incoherent scatter radar density measurements over Jicamarca, *J. Geophys. Res.*, *110*, A12314, doi:10.1029/2005JA011438.

Chau, J. L., M. A. Milla, and E. Kudeki (2010), Multi-frequency radar studies of the equatorial 150-km region, in *Proceedings of the Twelfth Workshop on Technical and Scientific Aspects of MST Radar*, edited by N. Swarnalingam and W. K. Hocking, pp. 165–168, Ottawa, Ont., Canada.

Choudhary, R. K., J.-P. St.-Maurice, and K. K. Mahajan (2004), Observations of coherent echoes with narrow spectra near 150 km altitude during daytime away from the dip equator, *Geophys. Res. Lett.*, *31*, L19801, doi:10.1029/2004GL020299.

Cosgrove, R., and T. Tsunoda (2002), A direction-dependant instability of sporadic E layers in the nighttime midlatitude ionosphere, *Geophys. Res. Lett.*, *29*18, 1864, doi:10.1029/2002GL014669.

de Paula, E. R., and D. L. Hysell (2004), The Säo Luís 30 MHz coherent scatter ionospheric radar: System description and initial results, *Radio Sci.*, *39*, RS1014, doi:10.1029/2003RS002914.

Dymek, M. K. (1980), Photochemical model of ion composition and electron density in the ionosphere at 70–300 km, in *Low Latitude Aeronomic Processes*, *COSPAR Symp. Ser.*, vol. 8, edited by A. P. Mitra, pp. 115–118, Pergamon, New York.

Kudeki, E., and C. D. Fawcett (1993), High resolution observations of 150 km echoes at Jicamarca, *Geophys. Res. Lett.*, *20*, 1987–1990, doi:10.1029/93GL01256.

Kudeki, E., C. D. Fawcett, W. L. Ecklund, P. E. Johnston, and S. J. Franke (1998), Equatorial 150-km irregularities observed at Pohnpei, *Geophys. Res. Lett.*, *25*, 4079–4082, doi:10.1029/1998GL900069.

Patra, A. K., and N. V. Rao (2006), Radar observations of daytime 150-km echoes from outside the equatorial electrojet belt over Gadanki, *Geophys. Res. Lett.*, *33*, L03104, doi:10.1029/2005GL024564.

Patra, A. K., and N. V. Rao (2007), Further investigations on 150-km echoing riddle using simultaneous observations of 150-km and *E* region echoes from off-electrojet location Gadanki, *J. Geophys. Res.*, *112*, A09301, doi:10.1029/2006JA012204.

Patra, A. K., P. B. Rao, V. K. Anandan, A. R. Jain, and G. Viswanathan (2002), Evidence of intermediate layer characteristics in the Gadanki radar observations of the upper *E* region field-aligned irregularities, *Geophys. Res. Lett.*, *29*(14), 1696, doi:10.1029/2001GL013773.

Patra, A. K., T. Yokoyama, Y. Otsuka, and M. Yamamoto (2008), Daytime 150-km echoes observed with the Equatorial Atmosphere Radar in Indonesia: First results, *Geophys. Res. Lett.*, *35*, L06101, doi:10.1029/2007GL033130.

Røyrvik, O. (1982), Drift and aspect sensitivity of scattering irregularities in the upper equatorial *E* region, *J. Geophys. Res.*, *87*, 8338–8342, doi:10.1029/JA087iA10p08338.

Røyrvik, O., and K. L. Miller (1981), Nonthermal scattering of radio waves near 150 km above Jicamarca, Peru, *J. Geophys. Res.*, *86*, 180–188, doi:10.1029/JA086iA01p00180.

Tsunoda, R. T. (1994), Enhanced velocities and shear in daytime E_{sq} over Kwajalein and their relationship to 150 km echoes over dip equator, *Geophys. Res. Lett.*, *21*, 2741–2744, doi:10.1029/94GL02507.

Tsunoda, R. T., and W. L. Ecklund (2000), On the nature of 150-km radar echoes over the magnetic dip equator, *Geophys. Res. Lett.*, *27*, 657–660, doi:10.1029/1999GL003689.

Tsunoda, R. T., and W. L. Ecklund (2004), On the summer maximum in the occurrence frequency of 150-km (F_1) radar echoes over Pohnpei, *Geophys. Res. Lett.*, *31*, L06810, doi:10.1029/2003GL018704.

Tsunoda, R. T., and W. L. Ecklund (2007), On the visibility and zenithal confinement of 150-km (F_1) radar echoes, *Geophys. Res. Lett.*, *34*, L21102, doi:10.1029/2007GL031276.

Tsunoda, R. T., and W. L. Ecklund (2008), On the sheet-like nature of 150 km (F_1) radar echoes, *Geophys. Res. Lett.*, *35*, L05102, doi:10.1029/2007GL032152.

Van Zandt, T. E., R. B. Norton, and G. H. Stonehocker (1960), Photochemical rates in the equatorial F_2 region from the 1958 eclipse, *J. Geophys. Res.*, *65*, 2003–2009, doi:10.1029/JZ065i007p02003.

A. K. Patra, National Atmospheric Research Laboratory, Gadanki 517 112, India. (akpatra@narl.gov.in)

P. Pavan Chaitanya, Department of Physics, Sri Venkateswara University, Tirupati 517 502, India.

D. Tiwari, Indian Institute of Geomagnetism, Navi Mumbai 410 218, India.